Practical Constraints on Nonlinear Transmission Lines for RF Generation

Elizete G. Lopes Rangel, *Member, IEEE,* José O. Rossi, *Senior Member, IEEE,* Joaquim J. Barroso, Fernanda S. Yamasaki, *Member, IEEE,* and Edl Schamiloglu, *Fellow, IEEE*

***Abstract*— Previous research has shown the applicability of nonlinear transmission lines (NLTLs) in high speed and wide bandwidth systems. These applications involve techniques for forming and sharpening a short electrical pulse to achieve pulse compressors, frequency multipliers, phase shifters, and, in addition, radio frequency (RF) generation, holding, in this case, a great potential for replacing vacuum electron tubes with a low cost and fully solid-state technology. Based on the analysis of relevant experimental results of different types of NLTLs reported in the literature, this paper presents an investigation about the correlation between the performance limits of NLTLs and specific characteristics of the materials used in their construction, concluding that there is a pressing demand for the development of high-performance dielectric and magnetic materials with special characteristics such as highly nonlinear behavior, low losses at microwave frequencies, and thermal stability that would allow for an improvement in the performance of NLTLs, enabling their operation at higher frequencies and with better electrical-to-RF conversion efficiency. The achievement of a stable behavior over a broader operating temperature range would allow the application of NLTLs in military and aerospace devices.**

***Index Terms*— Ferrimagnetic material, ferrite, ferroelectric material, nonlinear transmission lines (NLTLs), RF generation, Schottky diode, soliton, varactor diode.**

I. Introduction

SINCE the 1970s, nonlinear transmission lines (NLTLs) have been the subject of several studies that have investigated their performance by means of mathematical analysis [1]–[3], computer simulation, and practical experiments that have shown their suitability for application in high speed and wide bandwidth systems. These applications involve techniques for pulse forming and sharpening which are applied in signal processing such as pulse compressor [4], [5], frequency multiplier [6], [7], phase shifter [8], [9], oscillator [10], [11], high-speed metrology [12], radar [13], defense electronic countermeasures (jamming) [14], electron beam driver [15], [16], and RF power generation [17]–[19], holding, in this case, a great potential for replacing vacuum electron tubes as a low cost and fully solid-state technology requiring no vacuum systems.

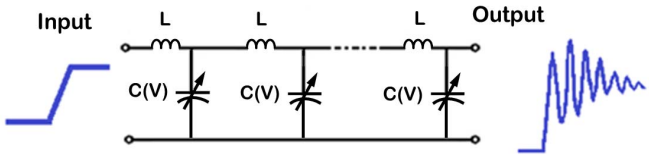

Fig. 1. Circuit model of a capacitive NLTL.

The generation of solitons (solitary pulses with a constant shape and velocity) can be obtained with three different types of NLTLs: 1) in a line where there is a balance between nonlinearity and dispersion; 2) through the effect of damped precession motion of magnetic dipoles moments in a line built with ferrimagnetic materials (ferrites) that are polarized with external magnetic field; and 3) in a line that exhibits anomalous dispersion and nonlinearity.

A discrete NLTL consists of a nonlinear dispersive medium where electrical solitons propagate in the form of voltage waves with a constant shape and velocity. Soliton formation occurs due to the balance between the effects of dispersion and nonlinearity. Dispersion arises from the periodic nature of the elements while the nonlinearity is introduced by nonlinear dielectric materials, such as voltage-dependent capacitors, and/or nonlinear ferrimagnetic materials, such as current-dependent inductors, which are arranged in a series of *LC* section low-pass filters. Indeed, this type of NLTLs can be categorized as capacitive, inductive, or hybrid lines according to the nonlinear elements used. A circuit model of a capacitive NLTL is shown in Fig. 1.

For a discrete NLTL, the general and traditional mathematical analysis of wave propagation is described by the solution of the nonlinear partial differential Korteweg-de Vries (KdV) equation (1) whose solution is given by the hyperbolic secant square function (2), when a linear capacitance behavior (3) is assumed [20]

$$\frac{\partial u}{\partial t} + 6u\frac{\partial u}{\partial x} + \frac{\partial^3 u}{\partial x^3} = 0 \tag{1}$$

$$u(x,t) = \frac{v}{2}\text{sech}^2\left[\frac{\sqrt{v}}{2}(x - vt - x_0\right] \tag{2}$$

$$C(V) = C_0(1 - bV) \tag{3}$$

Manuscript received December 28, 2017; revised May 11, 2018 and August 15, 2018; accepted October 11, 2018. This work was supported in part by SOARD-USAF under Contract FA9550-18-1-0111 and in part by AFOSR-UNM under Contract FA9550-15-10094. The review of this paper was arranged by Senior Editor W. Jiang. *(Corresponding author: Elizete G. Lopes Rangel.)*

E. G. L. Rangel, J. O. Rossi, and F. S. Yamasaki are with the Plasma Laboratory, National Institute for Space Research, 12227-010 São José dos Campos, Brazil (e-mail: elizete.rangel@inpe.br; jose.rossi@inpe.br; fernandayamasaki@hotmail.com).

J. J. Barroso is with the Division of Electronic Engineering, Technological Institute of Aeronautics, 12228-900 São José dos Campos, Brazil (e-mail: barroso@ita.br).

E. Schamiloglu is with the Department of Electrical and Computer Engineering, University of New Mexico, Albuquerque, NM 87131-0001, USA (e-mail: edls@unm.edu).

Color versions of one or more of the figures in this paper are available online at http://ieeexplore.ieee.org.

Digital Object Identifier 10.1109/TPS.2018.2876020

where x_o is the initial space position (phase) and ν is the wave propagation velocity, noting that (2) shows the dependence of the amplitude of solitons on their velocity. $C(V)$ is the capacitance as a function of the applied voltage and C_0 and b are the initial capacitance and a constant coefficient, respectively.

The approach of using the KdV equation as the approximate partial differential equation governing the behavior of discrete NLTLs was discussed in [1], where Nikoo and Hashemi presented the exact nonlinear partial differential equation (4) which has soliton solutions showing the well-known properties of the KdV solitons (5) and adopting a more realistic model for the capacitor nonlinearity (6)

$$\frac{d^2F[V(n,\tau)]}{d\tau^2} = V(n+1,\tau) - 2V(n,\tau) + V(n-1,\tau) \quad (4)$$

$$V(n,t) = A\ \text{sech}^2\left(\frac{0.96t}{\sqrt{L_0C(A)}} - 1.605n\right) \quad (5)$$

$$C(V) = \frac{C_0}{\sqrt{1+V/V_J}}. \quad (6)$$

Validated through the comparison with simulation and experimental results, this mathematical model has shown to be suitable for both nonlinear capacitors and varactors [1]. In (4), the nonlinearity is represented by the functional $F[V(n,\tau)]$ on the left-hand side, $V(n,\tau)$ is the time-dependent voltage at the nth node of the line, τ is the normalized time, A is the peak voltage, L_0 is the linear inductance, C_0 is the capacitance without bias, $C(V)$ is the voltage-dependent capacitance, V is the applied voltage, and V_J is a constant.

The nonlinear property sharpens the rise time as the pulse propagates along the line while dispersion causes the pulse to breakup into multiple sinusoidal oscillations as harmonic components propagate at different speeds. There are three basic equations for describing the discrete LC ladder network: the phase velocity v_p, the characteristic impedance Z_0, and the cutoff frequency f_c, also called the Bragg frequency because of the similarity to Bragg diffraction in optics, which corresponds to a phase shift of 180° per stage. These equations are given as follows:

$$v_p = \frac{1}{\sqrt{(L(I)C(V))}} \quad (7)$$

$$Z_0 = \sqrt{\frac{L(I)}{C(V)}} \quad (8)$$

$$f_C = \frac{1}{\pi\sqrt{(L(I)C(V))}} \quad (9)$$

where $L(I)$ is the inductance as a function of current and $C(V)$ is the capacitance as a function of voltage.

The voltage modulation depth (VMD) is a useful parameter for comparing pulses with ac and dc components as a means to quantify the level of modulation. The VMD is often defined as the average peak-to-trough load oscillation voltage (V_{avg}) for the first three pulse cycles [21]

$$\text{VMD} = V_{\text{avg}} = \frac{\sum_{j=1}^{3}(V_{\text{pt}})_j}{3} \quad (10)$$

where j is the oscillation cycle number and V_{pt} is the peak-to-trough load voltage. Accordingly, the average power (P_{avg}) for the first three RF cycles can be expressed in terms of VMD as [21]

$$P_{\text{avg}} = \frac{(\text{VMD}/2)^2}{R_L} \quad (11)$$

where R_L is the resistive load. In NLTLs, the RF power output calculated from the VMD is much lower than the peak instantaneous power as the waveform has a large dc component. While most of the input power is well matched to the NLTL input impedance, typically 20% of this power is converted to the output RF power [22] since RF power includes high-frequency power components not present in the input pulse [23].

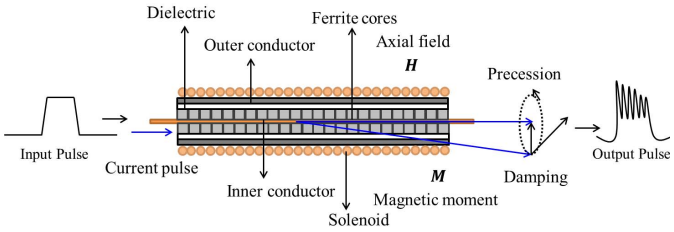

Fig. 2. Block diagram of a gyromagnetic NLTL showing the precession of the magnetic moments M in the ferrite. Reproduced from [26], 978-1-5090-6241-6/17 © 2007 IEEE.

NLTLs can operate in either pulse sharpening or microwave generating modes. In a capacitive NLTL, the operating mode depends on the pulse rise time reduction caused by the LC elements, as well as on the rise time of the input pulse. A rough estimative for the pulse rise time reduction (ΔT) caused by the LC ladder sections can be made by calculating the time delay difference between the lower amplitude portion and the peak of the propagation pulse which is described in [24] as

$$\Delta T = t_{\text{ri}} - t_{\text{ro}} = n(\sqrt{LC_0} - \sqrt{LC(V_{\text{max}})}) \quad (12)$$

where t_{ri} is the input rise time, t_{ro} the output rise time, n is the number of sections, and V_{max} is the maximum voltage applied to the capacitor. When the rise time t_{ri} is larger than ΔT, only pulse sharpening occurs. On the other hand, for the case $t_{\text{ri}} < \Delta T$ and since the rise time is limited to $1/f_c$, the propagating pulse is broken into a train of solitons (Fig. 1) rather than simply pulse sharpening. In a discrete capacitive NLTL the number of sections, the fractional change in the nonlinear capacitance, the frequency-dependent losses and the characteristics of the input signal (amplitude, frequency, duty cycle, and rise time) establish the signal propagation behavior along the line [23], [25].

The gyromagnetic line is another type of NLTL that consists of a continuous and nondispersive medium formed by a coaxial transmission line loaded with ferrite-based magnetic cores immersed in a constant external axial magnetic field (Fig. 2).

In a gyromagnetic NLTL, the microwave oscillations arise from the damped gyromagnetic precession of the spin magnetic moments of the electrons and are reinforced by the nonlinearity of the ferrimagnetic material. The high-frequency precession in the ferrite induces a high-frequency oscillation on the pulse as it travels through the NLTL. The resulting pulse at the output of the NLTL has the form of the input

pulse but with superimposed RF oscillations. The frequency of the precession is dependent upon the axial magnetic field, the input voltage, load impedance, and the magnetic properties of the ferrite material [27].

An incident high-voltage pulse disturbs the magnetic moments in the azimuthal direction and causes their precession. The precession motion of magnetic dipole moments is mathematically described by the Landau–Lifshitz–Gilbert equation [17], [26]

$$\frac{\partial \mathbf{M}}{\partial t} = -\gamma\,\mu_0[\mathbf{M}\times\mathbf{H}_{\text{eff}}] + \frac{\alpha}{M_S}\boldsymbol{M}\times\frac{\partial \boldsymbol{M}}{\partial t} \tag{13}$$

where μ_0 is the magnetic permeability of free space, γ is the electron gyromagnetic ratio ($1.760\times10^{11}\text{rad}\cdot\text{s}^{-1}\text{T}^{-1}$), α denotes the Gilbert phenomenological damping factor which is characteristic of the material, with typical values in the range of $0.001-0.1$, and M_S is the static magnetization at saturation. The first term on the right-hand side of (13) represents the precession motion of the magnetization vector ($\mathbf{M}$) around the effective magnetic field ($\boldsymbol{H}_{\mathbf{eff}}$), which results from the interaction of the axial biasing field and azimuthal incident field. The second term on the right-hand side of (13) is the damping term, which reduces the precession angle and causes the alignment of the magnetic moment with the external magnetic field.

The duration of the output RF pulse produced by NLTL is mainly limited by the relaxation time of gyromagnetic precession, which is represented by the second term on the right-hand side of (13) and is usually of the order of several ns. The high-voltage input pulse must have a rise time shorter than the precession relaxation time to excite an RF pulse. Because of this, experiments with gyromagnetic NLTLs require an input pulse with the rise time of the order of 2–3 ns. Furthermore, in gyromagnetic lines, the relaxation time of the magnetic spin, which is in the range of 2–3 ns, bounds the lower output frequency at around 300–500 MHz as the period of oscillations should not be higher than the relaxation time [17].

To evaluate the upper frequency, we note that the precession frequency of a gyromagnetic NLTL can be estimated as [26]

$$f = \frac{\gamma}{2\pi}\left(\frac{\mu_0}{\chi}M_s - \mu_0 H\right) \tag{14}$$

where in SI units, $\gamma/2\pi \approx 28$ GHz/T, the magnetization of ferrite at saturation $\mu_0 M_S = 0.35$T, $\mu_0 = 4\pi\times10^{-7}$ H/m, with H given in A/m; the azimuthal magnetic susceptibility χ is a dimensionless parameter which varies with the azimuthal field generated by the line pulse current, which in turn depends on the peak of the input pulse applied. The first term on the right-hand side of (14) becomes much larger than the second one if χ is small, which occurs when the ferrite saturates in the presence of a strong azimuthal magnetic field. By neglecting the second term and if χ decreases to no less than unity at ferrite saturation, the maximum expected frequency to be generated from a gyromagnetic line would be of the order of 9.8 GHz (= 28 GHz/T × 0.35 T). This reasoning is based on the fact that χ never goes to zero since the relative permeability (μ_r) of ferrite never drops below 2 during saturation at most, noticing that $\chi = \mu_r - 1$. In fact, the above estimate is consistent with frequencies of 6 GHz experimentally measured in [50].

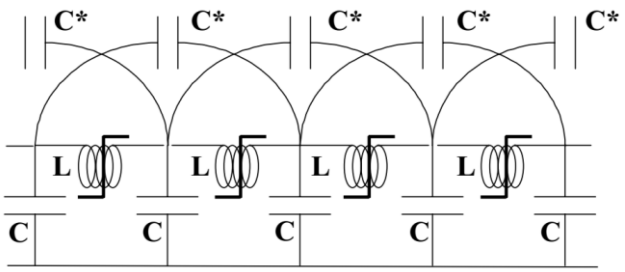

Fig. 3. Synchronous wave NLTL. Reproduced from [30], 1-4244-0914-4/07 © 2007 IEEE.

Gyromagnetic NLTLs can either operate in pulse sharpening or microwave generating mode depending on the initial magnetization of the ferrimagnetic material and the applied magnetic field. The magnetic biasing of ferrimagnetic materials is achieved by an axial magnetic field produced by an external solenoid or permanent magnets that align the magnetic moments of the ferrite material along the axis of propagation. Under the application of a high-voltage input pulse, an azimuthal magnetic field is generated, and if sufficiently strong, saturates the ferrite quickly, reducing its permeability. The decreased permeability increases the phase velocity of the propagating wave. The peak of the pulse will then travel faster than its lower amplitude components. The propagation velocity in a nonlinear magnetic medium is given by [28]

$$v_p = \frac{c}{\sqrt{\varepsilon_r \mu_r(I)}} \tag{15}$$

where c is the speed of light in vacuum and ε_{r} and μ_{r} are the relative permittivity and the relative magnetic permeability of the medium, respectively. As the leading edge of the input pulse with higher amplitude travels faster than the portion with smaller amplitude, the emerging output pulse is sharpened. In this case, the pulse rise time reduction at the output of the line is estimated by [28]

$$\Delta T = \sqrt{LC} - \sqrt{L_{\text{sat}}C} \tag{16}$$

where L is the coaxial line inductance far from saturation, L_{sat} is the saturated inductance of coaxial line, and C is the coaxial line capacitance. The pulse rise time reduction is limited by the switching characteristics of the ferrite due to the time it takes to switch from one state to another on the B–H curve of the material, which is related to the magnetization relaxation process in the magnetic material.

Another topology of NLTLs described in the literature is called the synchronous wave NLTL, in which the propagation of the shock waves occurs due to the combination of the anomalous dispersion and the magnetic nonlinearity. Fig. 3 illustrates the configuration of a planar synchronous wave NLTL, where the cross-linked capacitors (C∗) produce the anomalous dispersion and the magnetic nonlinearity is obtained with polarized inductor ferrites.

The synchronous wave NLTL can have planar or coaxial geometry [30]–[32] and is based on the synchronism between the RF wave phase velocity (v_p) and the shock wave

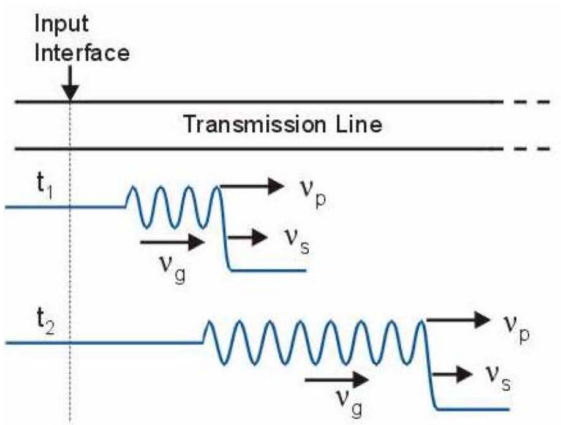

Fig. 4. RF formation in a synchronous wave NLTL. Reproduced from [30], 1-4244-0914-4/07 © 2007 IEEE.

velocity (v_s), making it possible to adjust the frequency of the oscillations by means of the phase velocity. Fig. 4 illustrates the propagation of RF oscillations produced along the saturated line, which was designed to present group velocity (v_g) of the RF wave less than its phase velocity (v_p).

The adjustment of the phase velocity is obtained by varying the magnetic bias of the ferrites. The phase of the RF oscillation produced is constant with respect to the shock wave, i.e., the shock wave consists of half of the first RF cycle. The energy flows from the shock wave to the RF oscillations that have a group velocity less than the velocity of the shock wave, which explains why the number of oscillations increases as the shock wave propagates along the line.

II. Research on NLTLs Based on Nonlinear Dielectric Materials

The literature reports the practical implementation of a capacitive NLTL in which the nonlinear components are made of a ferroelectric dielectric. Commercially available ferroelectric materials are found in some ceramic capacitors that exhibit a capacitance change when subjected to a great variation of voltage. A few researchers [19], [33], [34] also reported the use of ceramic blocks specially manufactured to use as a nonlinear dielectric in NLTLs, which also require the application of higher input voltages in the range of several kV.

A. Characteristics of Nonlinear Dielectric Materials Used in NLTLs

Ferroelectric materials are characterized by having two phases: paraelectric (or nonpolar) and ferroelectric (or polar). In the first, the polarization of the material has a linear behavior when subjected to an external electric field and the oriented dipoles return to their original states when the field is removed. In addition to being nonlinear, in the ferroelectric phase there is a spontaneous electric polarization that can be reversed by the application of a strong external electric field and, as a result, the relative permittivity (dielectric constant) in the ferroelectric phase can vary by the application of an external electric field. These materials usually present high values of electric permittivity which are temperature dependent

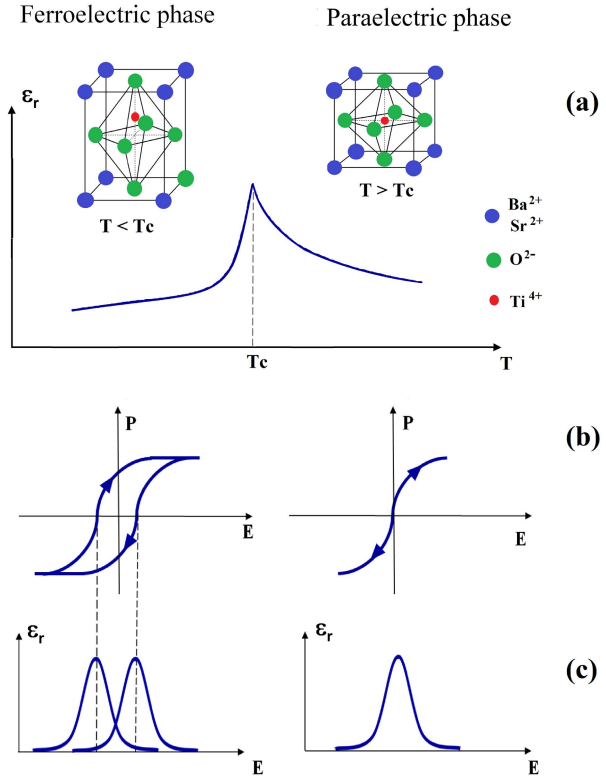

Fig. 5. Phase transformation of a ferroelectric material at the Curie temperature (a) crystalline structure, (b) polarization response with applied electrical field, and (c) relative permittivity behavior with applied electrical field.

due to the well-known structural phase transition at the Curie temperature (T_c), as pictured in Fig. 5(a).

The spontaneous polarization arises from the symmetry breaking of the crystalline structure, whose switching under an external electric field results in a typical ferroelectric hysteresis loop. The hysteresis loop changes with temperature (T) and undergoes a phase transition as the temperature is increased [see Fig. 5(a) and (b)]. The dependence of the polarization (P) and the corresponding relative permittivity (ε_r) on the applied electric field (E) plotted in Fig. 5(b) and (c), respectively, for both the ferroelectric and paraelectric phases, show that there is a nonlinear relation between polarization and electrical field, which gives rise to the electrically tunable relative permittivity, also called dielectric constant.

The dielectric losses in ferroelectric materials arise from conduction losses (ohmic conductivity), hysteresis losses (denoted by the area enclosed within the P–E loop) and relaxation losses (reorientation of the electric dipoles in response to an alternating electric field). Dielectric losses cause the degradation in the performance of an NLTL by reducing its conversion efficiency and limiting its operating frequency.

The nonlinear characteristic of ferroelectric materials finds application in the construction of NLTLs but requires the control of several factors that effectively enable the access of the nonlinearity of ferroelectric materials: 1) the Curie temperature of the compound should be near the operating temperature (room temperature) to allow operation of the dielectric in

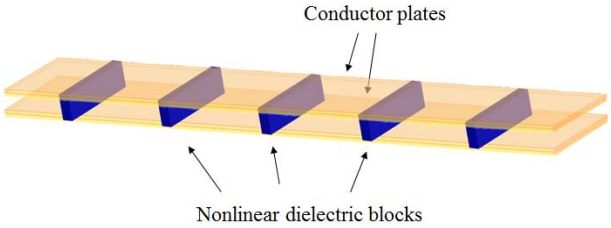

Fig. 6. Illustration of a capacitive NLTL in a parallel-plate shape loaded with ferroelectric nonlinear dielectrics.

its paraelectric phase, where depending on the material it can present a strong nonlinearity; 2) the breakdown voltage should be high enough to allow achieving higher nonlinearity of the dielectric, that is, to obtain the required variation of the capacitance across the range of applied voltage; and 3) low dielectric losses in the radio frequency (RF) range at least at a repetition pulse rate in the tens of hertz without external cooling.

B. NLTLs Built With Ceramic Blocks

Surveys report the investigation of dispersive NLTLs using a nonlinear dielectric in a parallel-plate design (see Fig. 6) with ceramic blocks made of ferroelectric compounds such as barium and strontium titanate [19] and [33], or lead magnesium niobate [34], which present an extremely high relative permittivity. To maximize the nonlinearity of these ferroelectric materials, they should be used near to the Curie temperature (around 120 °C barium titanate) and to be exposed to an electric field variation of the order of kilovolts. The permittivity and the relaxation frequency of a dielectric material are dependent on additives and processing techniques during manufacture. Unfortunately, the investigation on the addition of compounds to the dielectric materials for maximizing the nonlinearity has shown an increase of the relaxation time of the electric dipole moments leading to an increase in dielectric losses, which, in turn, prevents the generation of oscillations in an NLTL [33].

Good results were obtained in [19] with the generation of 10-MW peak power at frequency around 300 MHz, using 24 slabs made of barium and strontium titanate ($Sr_{0.4}Ba_{0.6}TiO_3$). This line was tested immersed in an oil bath with a termination load of 5 Ω, and fed with a single shot pulse input signal of 14 kV/50 ns. This line showed an average power conversion efficiency of 10%. The production of 60-MW peak power around 200 MHz is reported in [34] by using ceramic blocks made of barium and strontium titanate ($Sr_{0.91}Ba_{0.09}TiO_3$). The electrical tests were conducted with the line cooled to 77 K using liquid nitrogen and fed with a single shot input pulse signal between 10 and 30 kV. In [35], the results of a parallel-plate NLTL constructed with ceramic slabs made of lead–magnesium–niobate are presented. This line was fed with input voltages from 4 to 43 kV and only showed the production of low-intensity solitons due to the dielectric losses associated with this material, which are macroscopically represented by a resistor in series with the variable capacitors in Fig. 1. Branch and Smith [33] reported the generation of shock waves with 10-kV amplitude and rise time of 410 ps in an NLTL built with ceramic blocks with composition $Ba_{0.75}Sr_{0.25}Ti_{0.95}Zr_{0.05}O_3$. In this experiment, the NLTL was fed by a single pulse of 10 kV terminated with a 1.9-Ω resistor, which was made from an aqueous copper sulfate solution.

C. NLTLs Built With Ceramic Capacitors

The ferroelectric ceramics used in the construction of discrete NLTLs consist of commercially available ceramic capacitors that exhibit nonlinear capacitance when a voltage is applied. For a commercial ceramic capacitor, the datasheet of the manufacturer only provides the change in capacitance with applied dc voltage. The reduction of capacitance with increasing voltage is not a property of all capacitors, but only applies to capacitors made of ferroelectric dielectrics like barium titanate constructed without the addition of dopants to control thermal stability and, as a result, their capacitance has both strong temperature and voltage dependences.

The generation of high-power pulsed signals with fast rise times is the main application of NLTLs using commercial ceramic capacitor as a nonlinear element and requires the use of high-voltage input signals to effectively obtain the desired nonlinear behavior. With the use of ceramic capacitors, the following constraints are observed [36].

1) The nonlinearity is achieved with capacitors with large temperature dependence, and the heat generation by the hysteresis losses must be considered.
2) The commercial ceramic capacitors are normally limited up to 5 kV rated voltages and have self-resonant frequencies (frequency at which the capacitor starts behaving like an inductor) in the hundreds of megahertz range. This is a limiting factor for high-power and high-frequency applications.
3) The phenomenon of aging in ceramic capacitors is well known, and the manufacturers usually quote an aging rate in terms of the reduction of the value of a capacitance as a logarithmic function of time, and this process tends to be accelerated when they are subjected to a high level of electric stress that is required to produce the nonlinear response.

Experimental results with high-voltage NLTLs were presented in [37] showing the generation of pulsed RF waveforms at tens of kV and frequencies from around 10 to 90 MHz. These NLTLs were built using obsolete ceramic capacitors that had an excellent capacitance ratio and were stacked to improve their voltage rating. Single pulses around 30 kV were generated to supply these lines. The whole assembly operated submerged in insulating oil.

A reduction of the rise time from 340 to 50 ns for an NLTL of 15 sections built with inductors of 1.5 μH and ceramic capacitors of 1.24 nF (nominal value) at zero applied voltage that showed a capacitance decrease of 63% for a 25-kV incident pulse was reported in [38]. A 10-section NLTL built with inductors of 1.6 μH and three ceramic capacitors of 2.2 nF with a breakdown voltage of 6 kV in a series configuration is presented in [38]. The higher operating voltage

produced by the series configuration allowed the application of an input voltage of 18 kV which led to an 82% decrease in nominal capacitance and a reduction of the input pulse rise time from 500 to 120 ns. The production of RF oscillations with frequency about 4 MHz and peak voltage of 800 V was also reported in [39] with a discrete capacitive NLTL built with inductors of 3.3 μH and commercial ceramic capacitors of 1 nF which showed a capacitance change of 62%. The generation of high-voltage oscillations is reported in [25] for an NLTL in a circular configuration, consisting of two boards with 24 sections in parallel, each line being the load of the other, sharing a common input. Built with ceramic capacitors of 10 nF and inductors of 1 μH and fed by a single-shot 12-kV pulse, this line produced oscillations with frequency of about 16 MHz and peak voltage of 45 kV.

III. Research on NLTLs Based on Semiconductor Materials

Several researches have reported the use of commercial semiconductor devices as the nonlinear element in NLTLs. The nonlinearity of these devices arises from the junction capacitance under a reverse bias. Typically, the operating voltage of these devices ranges from few volts for silicon varactors diode and can reach the value of 3.3 kV for carbide silicon Schottky diodes. Therefore, by using these diodes in stacked configuration, an upper bound above 3.3 kV can be reached in high-voltage NLTLs. Besides the lumped lines, these capacitive NLTLs can be constructed with compact dimensions using different forms of planar transmission lines such as microstrip line, slot line, coplanar waveguide (CPW), and finline.

A. Characteristics of Semiconductor Diodes Used in NLTLs

The literature reports the construction of capacitive NLTLs using three different types of diodes that exhibit nonlinear capacitance with reverse applied voltage, which are varactor diodes, heterostructure barrier varactors (HBVs), and Schottky diodes. These devices have different characteristics due to their different construction and materials employed. A capacitive NLTL built with these diodes would have its performance directly influenced by the diode reverse breakdown voltage, the cutoff frequency, and the capacitance ratio.

In a diode, the depletion region, which is formed at the p-n junction under a reverse voltage polarization, gives rise to a junction capacitance. All diodes exhibit this variable junction capacitance, but varactors are manufactured to exploit this effect and to increase the capacitance variation. Unfortunately, as diode doping profile is made more abrupt the cutoff frequency also decreases [40]. Varactor diodes are used to construct low voltage capacitive NLTLs.

A Schottky diode is a semiconductor diode formed by the junction of a semiconductor with a metal. This diode presents a higher power handling capability, low power loss, low forward voltage drop, and a very fast switching action.

HBV diodes exhibit symmetric capacitance–voltage and asymmetric current–voltage characteristics. This leads to the generation of only odd harmonics of an applied signal since the even harmonics are canceled due to the symmetric nature of the nonlinearity, so they are used to build NLTLs that operate as frequency multipliers [6].

The capacitance of diodes that exhibit nonlinear behavior in the reverse state can be controlled by changing the bias. Junction capacitance change (C_J) arises from the variation of the charge carriers in the depletion layer in the p-n region and the C–V relation can be approximated by [25]

$$C_J = \frac{C_0}{(1 + V/V_J)^n} \tag{17}$$

where C_0 is the unbiased capacitance, V is the applied voltage, V_J is the junction voltage, and n is a grading coefficient related to the device doping profile (concentration of carriers) which express the voltage sensitivity of C_J. Besides the voltage–capacitance relation, another important figure of merit of a varactor is the cutoff frequency (f_c) which is described by [41]

$$f_c = \frac{S_{\max} - S_{\min}}{2\pi R_s} \tag{18}$$

where $S_{\max}$ and $S_{\min}$ are the maximum and minimum differential elastances (inverse of capacitance), respectively, during a pump cycle and R_s is the parasitic series resistance. For high efficiency, any varactor diode must exhibit low series resistance Rs and must accommodate a large elastance swing, i.e., a high $S_{\max}/S_{\min}$ ratio.

The minimum pulse rise in an NLTL is determined by the Bragg frequency (9), and for pulse propagation in an NLTL it is required that the diode cutoff frequency be higher than the Bragg frequency. A shock wave will result if the pulse rise time is lower than the inverse of the Bragg frequency. The cutoff frequency is defined as the frequency at which the capacitive reactance is equal to the series resistance. It is also a function of voltage, achieving its maximum value at the breakdown voltage, being an important consideration in diode selection. Ultimately, the minimum pulsewidth which may be generated on an NLTL is limited by the diode cutoff frequency and the total line loss [42].

The oscillation depth and total number of solitons generated can be increased by varying the nonlinearity and the total number of stages; however, the conductive and dielectric losses will dissipate much of the energy of the oscillations. This can significantly reduce the overall efficiency of the lines with many stages [22].

B. Lumped NLTLs With Varactors

Research on low-voltage NLTLs using varactors allows the investigation of parameters that affect their performance since the test equipment needed to perform these experiments are easily found in electronics labs. Fig. 7 shows a 60-section NLTL assembled on a PCB with surface mounted varactors and inductors.

The experimental results with low-voltage NLTLs were presented in [37], reporting the generation of pulse bursts at frequencies ranging from a few megahertz to 250 MHz. These lines were constructed using varactors diodes (BB212) and specially manufactured inductors (air cored and wound in-house).

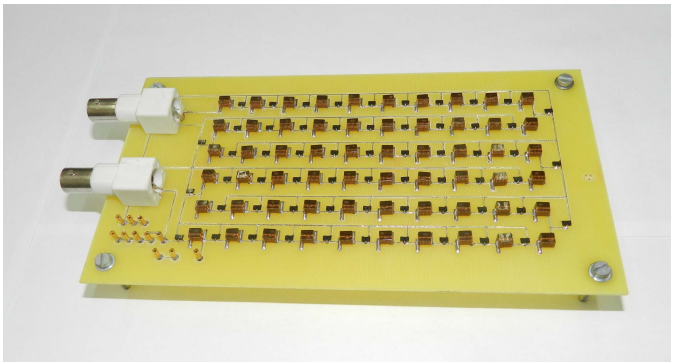

Fig. 7. Capacitive NLTL assembled in a PCB with surface mounted devices.

The results of research on low-voltage capacitive NLTLs built with varactors and inductors assembled on PCBs reported the generation of pulses on the order of 100 V with a rise time of 10 ns [25]. This 48-section NLTL employed inductors of 1 μH and low-voltage varactors (1N5822). The diodes presented a capacitance variation between 400 and 70 pF, when subjected to voltage pulses of the order of 40 V.

Another project investigated the performance of a 30-section capacitive NLTL constructed with inductors of 2.7 μH and varactor diodes (BB809). This line resulted in RF signal generation of the order of 33 MHz [23], concluding that the propagation of the signal along the line is influenced by several factors such as the capacitance rate variation (77%), frequency-dependent losses, and characteristics of the input signal (amplitude, shape, rise time, frequency, and duty cycle).

Elizondo-Decanini *et al.* [25] pointed out that the strays on a nonlinear line assembled on a PCB dominate the minimum capacitance value. In fact, in NLTLs built with varactor diodes up to 200 V, the frequency limit is about 250 MHz, causing above 300-MHz stray impedances in the lumped NLTL which seriously impair the performance of the line and RF formation dies away [29].

C. Monolithic NLTLs Using Varactors Schottky and HBV Diodes

Since the 1990s, several researchers have reported the construction of monolithic NLTLs, which enables the construction of very compact NLTLs structures loaded with Schottky or HBV diodes that are fabricated in a semiconductor substrate. These semiconductors have very high cutoff frequency (THz) but have a breakdown voltage of less than 10 V, allowing the construction of low-voltage NLTLs.

Rodwell *et al.* [40] reported the construction of a monolithic NLTL built with a CPW structure loaded by reverse-biased gallium arsenide (GaAs) Schottky diodes at spacing d, as shown in Fig. 8. The experiments generated electrical step functions of about 5-V magnitude and with less than 1.4 ps of fall time, which allowed for the development of sampling circuits with bandwidth around 300 GHz. The authors pointed that in a CPW structure the circuit layout introduces a parasitic series inductance and shunt capacitance at the diode locations. However, CPW skin loss is a major parasitic parameter that must be minimized.

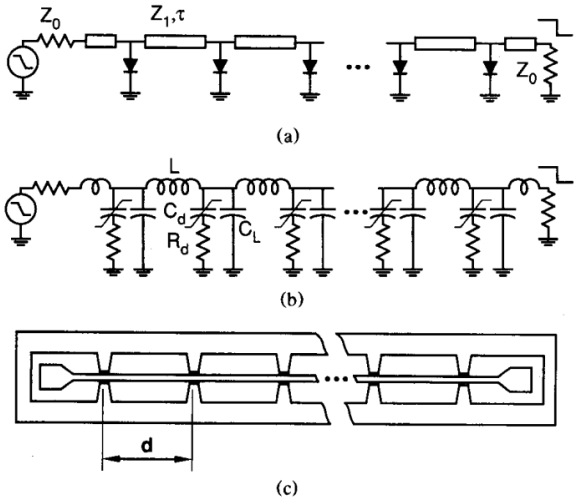

Fig. 8. Illustration of a monolithic GaAs nonlinear transmission line (a) circuit diagram, (b) equivalent circuit, and (c) layout. Reproduced from [40], 0018-9480/91/0700-1194 © 1991 IEEE.

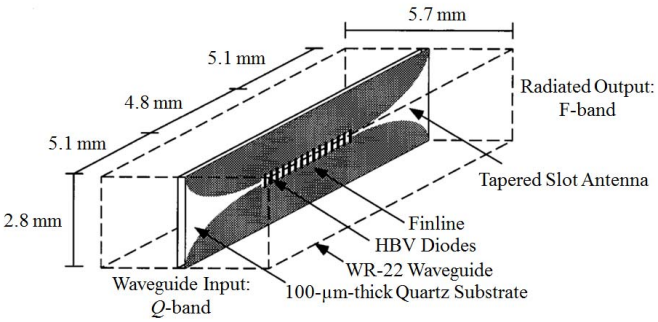

Fig. 9. Layout of a monolithic nonlinear transmission line constructed with a finline structure periodically loaded with HBV diodes. Adapted from [6], 1051–8207/00 © 2000 IEEE.

An NLTL implemented in a 90-nm CMOS technology is reported in [5], with a supply voltage of 1.2 V this line showed the compression of the input pulse from 37 to 14 ps (62%). The construction of a monolithic NLTL was presented in [6]; this NLTL consists of 15 discrete GaAs-based HBV diodes periodically soldered across a finline transmission line with tapered slot couplers at the input and output (Fig. 9). The HBV diodes presented a capacitance variation of 74% (6.8 pF/26 pF). This line worked as a frequency multiplier and exhibited 10-dBm peak radiated power at 130.5 GHz with more than 10% frequency tunability at the 3-dB bandwidth and 7% conversion efficiency. Another frequency tripler using InP-based HBV diodes in stacked configuration showed an output power of 10 dBm with an efficiency of 12% at 247 GHz [7].

Using diodes with variable capacitance in embedded coplanar or microstrip line, it is possible to achieve frequency in the GHz range, but with extremely low power. For very high Bragg frequencies, diode areas and spacing become impractically small, and parasitic effects can dominate the cell. Dissipation is also an issue for very high Bragg frequency lines since waveguide dimensions must become very small [43].

Experimental results of an NLTL constructed with silicon carbide (SiC) diodes (C4D05120E) are reported in [25]. This 24-section NLTL was assembled on a PCB using 1-μH

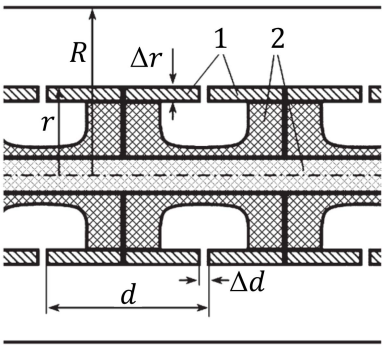

Fig. 10. Geometry of the periodic gas gap structure: (1) electrodes and (2) dielectric. Adapted from [44], 0093-3813 © 2007 IEEE.

inductors and diodes which showed capacitance variation from 380 to 40 pF for an input voltage of 100 V. A peak voltage of 700 V with oscillations was obtained at the output for a circular configuration.

Experiments [15] with an NLTL-based beam modulator generated an output signal with peak voltages around 1 kV, an average current from 1 to 3 mA, and with a pulsewidth around 2 ns at a frequency of 100 MHz. This NLTL was made of 78 sections mounted in a PCB using inductors of 120 nH and reverse-biased SiC Schottky diodes (C2D05120A).

IV. Research on NLTLs Based on Periodic Gas Gap Structure

The experimental results on the generation of high-voltage RF pulses using a 12-section periodic gas gap structure are reported in [44]. This NLTL has a coaxial geometry in which the inner cylindrical conductor sections are separated by gas-discharge gaps (Fig. 10) which cause the delay time of breakdown to exhibit a nonlinear dependence on the amplitude of the applied field, and so the central frequency in the pulse spectrum is a function of the amplitude of the incident TEM wave. The radius of the central stainless-steel conductor of the line was $r = 59$ mm, and the radius of the outer conductor was $R = 100$ mm. The dielectric structure was fabricated from polyethylene. The impedance of the line was 32 Ω.

The microwave generation occurs through successive breakdowns of overvoltage gas gaps producing an output signal which consists of an in-phase composition of RF fields produced by currents in the periodic gas gap structure of the inner conductor. Experiments were carried out in a chamber with the line filled with pure nitrogen that allowed the control of pressure between 1 and 20 atm. The central frequency of RF oscillations could be tuned by the gas pressure, with a range of optimum pressures leading to an energy conversion of around 10%. The line was driven by a pulse generator that provided 50 to 250 kV at a maximum repetition rate of 100 Hz. Experiments were carried out both with a matched resistive load and with RF irradiation into the free space by a horn antenna. The authors reported a most stable and efficient narrow-band operation (0.83–1.12 GHz) of the system with 12 cylindrical gas gaps producing an RF pulse of 200 kV at 1 GHz and an RF power of several hundreds of megawatts.

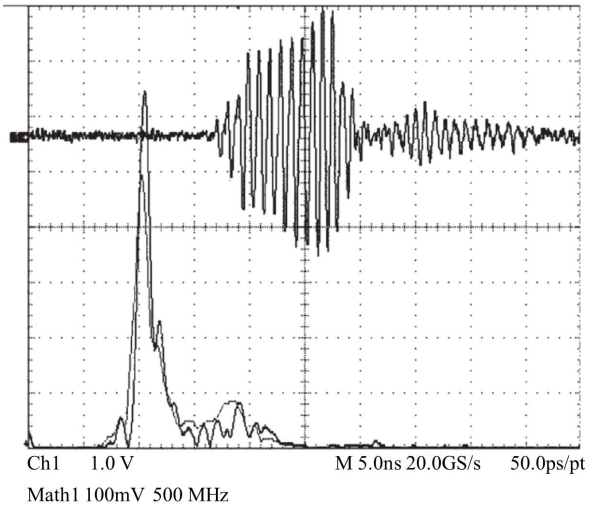

Fig. 11. NLTL with periodic gas gap structure: signal from the wideband receiving antenna (5 ns/div) and the FFT spectrum below (500 MHz/div). Adapted from [44], 0093-3813 © 2007 IEEE.

Fig. 11 shows a typical waveform of the RF pulse taken by the receiving dipole antenna 3 m away from the horn antenna for 12 discharge gaps with a period $d = 110$ mm, annular gaps Δd of 4 mm, pressure of 4.7 atm, and supply voltage of 175 kV.

V. Research on NLTLs Based on Ferrimagnetic Materials

Research on the construction of coaxial-based NLTLs loaded with ferrimagnetic materials report the use of ferrites beads and inductors made of windings in ferrite cores. The gyromagnetic properties of ferrites induce high-frequency oscillations which are reinforced by the nonlinearity in synchronous wave and gyromagnetic NLTLs.

A. Ferrimagnetics Materials

The macroscopic magnetic properties of a magnetic material are a consequence of interactions between an external magnetic field and the magnetic dipole moments of the constituent atoms. The relative magnetic permeability (μ) is defined as the ratio of magnetic flux density (B) to magnetic field intensity obtained from the slope of the B/H curve.

Ferrimagnetic materials are characterized by having domains in which the molecular magnets moments are already aligned. When a magnetic field is applied the domains progressively align with it. During this magnetization process, energy barriers must be overcome, giving rise to a hysteresis loop, as shown in Fig. 12.

Hysteresis in magnetic materials means lagging of the magnetization behind the magnetizing field and represents the losses when the material subjected to an alternating magnetic field. These losses arise due to the limit of magnetization switching frequency. In the B/H curve, the area of the hysteresis loop is associated with core losses, which increase in direct proportion to frequency, since each cycle traverses the hysteresis loop.

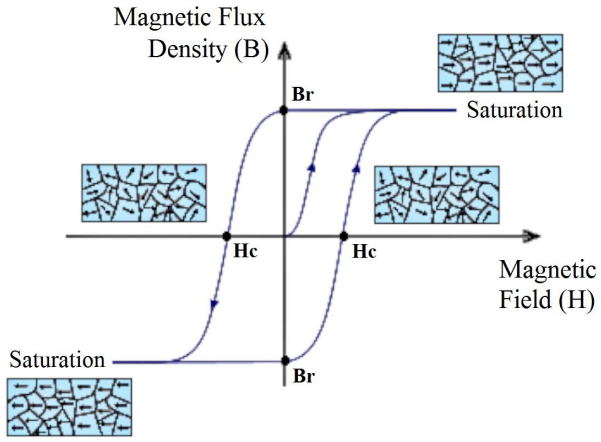

Fig. 12. Hysteresis loop of a ferrimagnetic material.

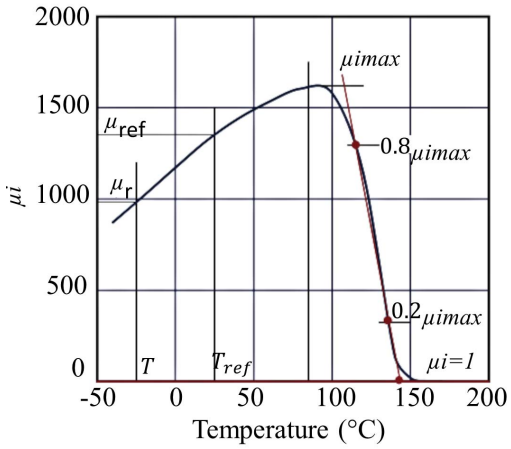

Fig. 13. Example of temperature change of permeability for a ferrite [45]. Adapted from [45], © 2018 TDK Corporation.

Another contribution to losses is the eddy currents which are induced in the core material by the time-varying magnetic flux; these currents, in turn, induce flux in opposition to the initial flux. Due to the high resistivity characteristic in the ferrimagnetic materials, eddy current losses in the core are usually much less than those due to hysteresis.

Ferrimagnetic materials are characterized by the temperature dependence of the magnetic properties. Above the Curie temperature, the ferrimagnetic materials undergo a phase transition and become paramagnetic, giving rise to a sharp change in magnetic properties due to the random orientation of magnetic moments. The behavior of permeability as a function of temperature is shown in Fig. 13. After reaching a maximum value at a certain temperature, the permeability of magnetic materials drops abruptly (coming to be equal to the permeability of free space, $\mu = 1$) as the temperature rises further.

Magnetic oxides can be classified as soft (magnetic core material), hard (magnet material), garnet and hexaferrite. The literature reports the use of soft ferrite and garnet ferrites in the construction of NLTLs due to its high initial permeability (μ_i), low coercivity (H_c), high intrinsic resistivity, and low hysteresis losses.

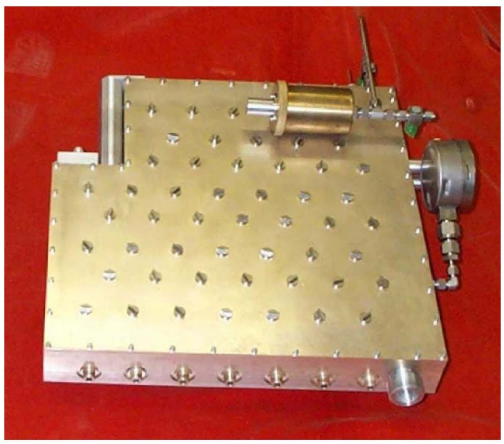

Fig. 14. Synchronous wave NLTL packaged in an aluminum box. Reproduced from [30], 1-4244-0914-4/07 © 2007 IEEE.

The magnetic properties of ferrites are strongly dependent on their chemical composition and on their microstructure. Soft ferrites have cubic spinel crystalline structure and their general composition is $MeFe_2O_4$, where Me represents one or several of the divalent transition metals, such as manganese, zinc, nickel, cobalt, copper, cadmium, iron, and magnesium. Commercial soft ferrites are usually composed by combinations of manganese and zinc (MnZn) and nickel and zinc (NiZn). Garnet ferrites have cubic centered crystalline structure and their chemical formula is $Me_3Fe_5O_{12}$, where Me is a trivalent ion such as a rare earth metal or yttrium.

B. Synchronous Wave NLTLs Using Ferrites

The investigation on synchronous wave NLTLs using axially biased ferrite and capacitive crosslinks is reported as a feasible technique to improve the performance of capacitive NLTLs, which present the decay of the amplitude of the oscillations (caused by losses) and wide frequency spectrum [46]. These lines are usually built with coaxial transmission line configurations, providing simple means of axial biasing and increased voltage handling capability.

Seddon *et al.* [30] presented the experimental results of a synchronous NLTL (Fig. 14) which produced 20-MW peak power with center frequencies from 200 MHz to 2 GHz that could be electronically tuned by adjusting the circuit parameters (L, C, C∗) and feeding a continuous dc bias current through the NLTL, which allows for the control of the initial state of the nonlinear inductors. This line was fed by an electrical input pulse of 30 to 50 kV, with a 10-ns rise time and a 50-ns flat top and can be operated in phased arrays. The transmission line is approximately 6 m long, but it was folded into a serpentine shape and enclosed in an aluminum box that is 0.5 m square and 0.07 m deep. To provide an electric insulation, the aluminum box was filled with insulating oil.

Another type of synchronous NLTL reported the construction of a line in a coaxial oil-insulated geometry [32] that generated RF with tunable frequency in the range of 0.9 to 1.5 GHz and instantaneous peak power on the order of 100 MW. This NLTL used an axial bias to control the shock

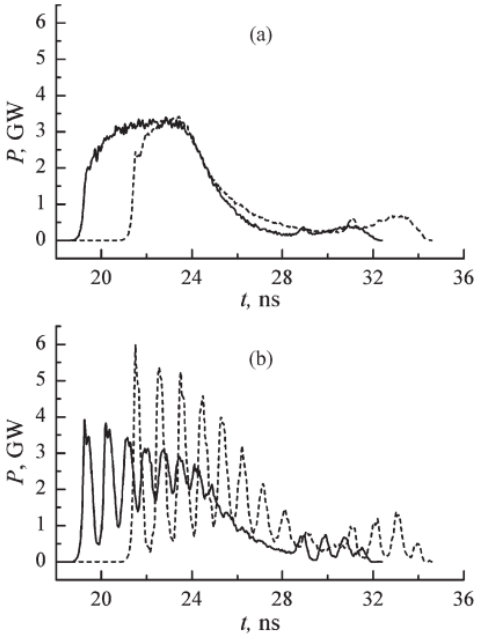

Fig. 15. Output power waveform for two lines of 41 cm (solid line) and 77 cm (dashed line) (a) with no external magnetic field and (b) H_0–40 kA/m. Reproduced from [44], 0093-3813 © 2007 IEEE.

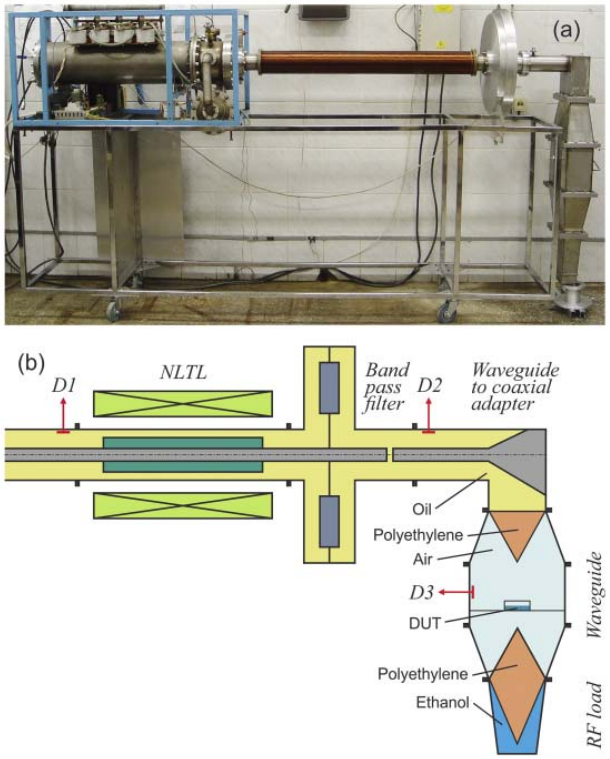

Fig. 16. (a) Photograph and (b) general schematic of the gyromagnetic NLTL RF source used in biological research. Reproduced from [47], with the permission of AIP Publishing.

speed and spatially dispersive geometric structure to provide a broad tuning range.

C. Gyromagnetic NLTLs

Recently researchers reported the generation of high-power RF using gyromagnetic NLTLs. These lines consist of a uniform coaxial line whose center conductor is encapsulated by ferrite beads. The biasing field can be provided by a solenoid wrapped around the NLTL or even by permanent magnets. The operational frequency can be controlled by varying the dimensions of the ferrimagnetic material, which affects the azimuthal magnetic field and material losses, or by varying the bias field strength.

The experimental results of two gyromagnetic NLTLs built with NiZn ferrite rings distributed with a step of 9 cm and length of 41 and 77 cm is reported in [44]. The experimental setup consists of two uniform sections filled with transformer oil and the NLTL between them. The NLTL was filled with transformer oil for increasing the electric strength. The maximum amplitude of the input voltage pulse was 295 kV. The performance of these lines was evaluated with the ferrites in both unsaturated and saturated condition. The saturated condition was achieved with the application of an external magnetic field ($H_0 \leq 80$ kA/m) generated by a dc solenoid. The experiments were conducted with a matched load and signals were measured with broadband capacitive dividers. Power waveforms at the load for the lines with 41 and 77 cm are shown in Fig. 15(a) and (b) for unsaturated and saturated condition, respectively.

The authors observed that increasing the ferrite section length decreases the pulse duration due to irreversible energy losses [Fig. 15(a)], while the power integral remains nearly constant with increasing the system length [Fig. 15(b)]. The energy conserved in the pulse propagating in the NLTL with saturated ferrite is indicative of a minor role of dissipative processes in the video to radio pulse energy conversion. With the ferrites in the saturated condition, the peak power of oscillations was around 700 MW with the voltage amplitude of 140 kV. The highest efficiency of power conversion for the maximum line length was estimated as 10%. The central frequency of oscillations could be adjusted from 0.6 to 1.1 GHz by varying the amplitude of the input voltage from 110 to 295 kV.

Romanchenko *et al.* [47] reported the development of a gyromagnetic NLTL source used in biological research which is illustrated in Fig. 16. This line produced RF pulses at frequencies from 0.6 to 1 GHz, with the ability to change the peak amplitude by about 400 times (52 dB), reaching a maximum value of nearly 40 kV/cm and decreasing to tens of V/cm. The experiments were performed using nickel zinc ferrite beads with saturation field $B_{\text{sat}} = 0.35$ T and coercivity $H_c = 410$ A/m. This NLTL was built in an air-filled waveguide and was fed by a driver which produced pulses with 9-ns width whose amplitude can be varied from 150 to 270 kV and optimal bias magnetic field of about 50 kA/m. The approximate length of this NLTL was about 1 m. This paper also reported on the investigation of the influence of both the ferrite and the NLTL diameter on the output depth modulation, and better results were achieved when the inner ferrite diameter almost coincided with the NLTL inner diameter. In this case, deeply modulated RF pulses were produced. The effect of the dielectric insulator on the performance of this line was also investigated. The insulator was used to prevent voltage breakdown between the inner and outer conductors,

where the incident pulse varied from 150 to 270 kV. The efficiency of RF generation of this gyromagnetic NLTL was evaluated for three types of insulators with different dielectric properties: SF_6 ($\varepsilon_r \approx 1$), vacuum pump oil ($\varepsilon_r \approx 2.15$), and castor oil ($\varepsilon_r \approx 4.05$). Better efficiency was obtained with vacuum pump oil. With SF_6, the efficiency was lower and there was a decrease in center frequency while for castor oil insulation the efficiency is strongly reduced, and the center frequency is increased. The reduction in efficiency for castor oil insulation was attributed to high dielectric losses, which results in the suppression of the NLTL pulse sharpening effect. The SF_6 insulation affects the wave velocities so that the reduced efficiency is probably caused by worsened conditions for synchronism between the phase and the electromagnetic shock wave velocity.

The investigation reported in [48] presented the construction of gyromagnetic NLTLs loaded with NiZn and MnZn ferrites. Due to the large electric fields found inside the NLTL, a fully encapsulating dielectric medium (SF_6 pressurized to 680 kPa) was used as an insulator to prevent breakdown. A secondary dc power supply provided the necessary current through a solenoid wrapped around the outer conductor of the NLTL to produce the axially directed, magnetic biasing field. By altering the bias magnitude, length of bias, and ferrite, the NLTL could be actively tuned for specific delay times. These NLTLs were fed by a single shot pulse around 30 kV. The line built with MnZn ferrite proved to be too lossy and did not produce microwaves, while the lines built with NiZn ferrites produced RF power of 4.8 MW with pulse lengths ranging from 1 to 5 ns and tuning frequency in the range of 2 to 4 GHz. The NiZn ferrites had different compositions; however, oscillations with higher amplitudes were achieved with ferrites that have relative permeabilities in the upper hundreds and saturation magnetizations around 3500 G. This paper also conducted an analysis of precession frequency of the ferrites using the ferromagnetic resonant spectroscopy (FMR) technique by measuring the resonance linewidth, which is directly related to the damping factor, concluding that for NiZn ferrites with different chemical compositions, the smaller the resonance linewidth (a parameter which is connected to the relaxation processes), the greater the amplitude of the oscillations. However, despite the MnZn ferrite having also presented a very narrow resonant linewidth, the NLTL built with this material did not produce oscillations due to its lower resistivity, which is 5–8 orders of magnitude lower than the NiZn ferrites.

Chadwick *et al.* [27] reported the construction of fully solid-state high-power microwave source that was built using a semiconductor opening switch diode as a pulse generator and a gyromagnetic NLTL. This structure produced peak output power about 90 MW and frequencies between 700 MHz and 1 GHz.

The suitability of yttrium iron garnet ferrites for use in gyromagnetic NLTLs was reported in [49]. The generation of microwave oscillations with peak power up to 200 kW was noted for an input signal of less than 6 kV with sub-nanosecond rise time. The resulting output of this NLTL was radiated, and field levels exceeding 1 kV/m at a target distance of 3 m at frequencies between 1.7 and 1.8 GHz were observed.

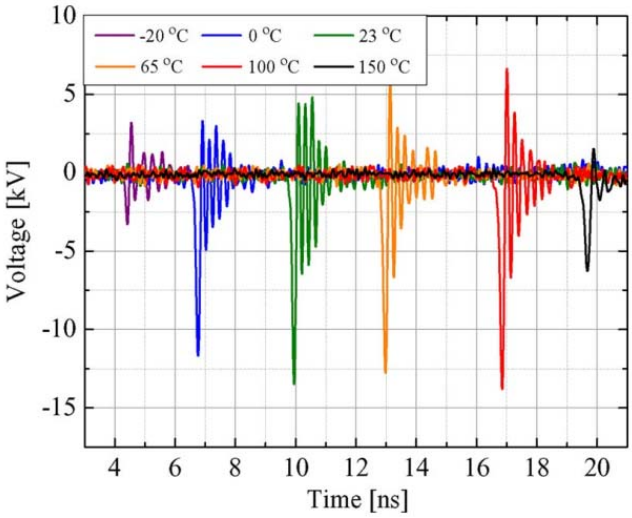

Fig. 17. Influence of the temperature on output oscillations of gyromagnetic line with 40-kV incident pulse and 19 kA/m bias. The shots shifting from left to right are increasing in temperature. For color copy: −20 °C—purple, 0 °C—blue, 23 °C—green, 65 °C—orange, 100 °C—red, and 150 °C—black. Reproduced from [50], 093-3813 © 2012 IEEE.

Bragg *et al.* [50] reported the temperature dependence of a ferrimagnetic-based NLTL that had been tested under the temperature range of −20 °C up to 150 °C. This temperature range covered a wide range of potential operating temperature and provided some insight into operational performance above the Curie temperature. The experiments were conducted with a single shot operation and the NLTL consisted of a coaxial line with toroidal ferrites loaded on the inner conductor. The experiments showed an increase of 50% in peak power relative to room temperature and a significant decrease of the frequency between 0 °C (maximum frequency obtained) and 100 °C, shown in Fig. 17. This paper concluded that the exact mechanisms responsible for power and frequency changes are not fully understood, and therefore, further experiments are needed to know the behavior of permeability, relaxation time, and switching time versus temperature.

The excellent result obtained with a gyromagnetic NLTL capable of producing RF pulses with estimated peak power of 260 MW at frequencies around 1 GHz with 100-Hz pulse repetition rate is described in [51].

The synchronized operation of four gyromagnetic NLTLs based on the parallel arrangement and loaded onto conical helix antennas is reported in [52]. The experiments showed that the radiation power density of synchronous four-channel operation is higher than for one-channel operation for 16 times. An effective potential of radiation of 360 kV at a center frequency of 2.1 GHz at a pulse repetition rate of 1 kHz was generated. The general schematic is depicted in Fig. 18(a). Four identical NLTLs (Fig. 18) had a length of 700 mm filling by NiZn ferrites with saturation $B\text{sat} = 0.4$ T and coercivity $H\text{c} = 80$ A/m.

This system was driven by RF source producing high-voltage pulses up to 500 kV. The transformer oil at five-bar pressure was used for NLTL insulation. Each NLTL was biased by five sectional solenoids, of which the first two sections were used for the delay control (about 300 mm of the ferrite filling),

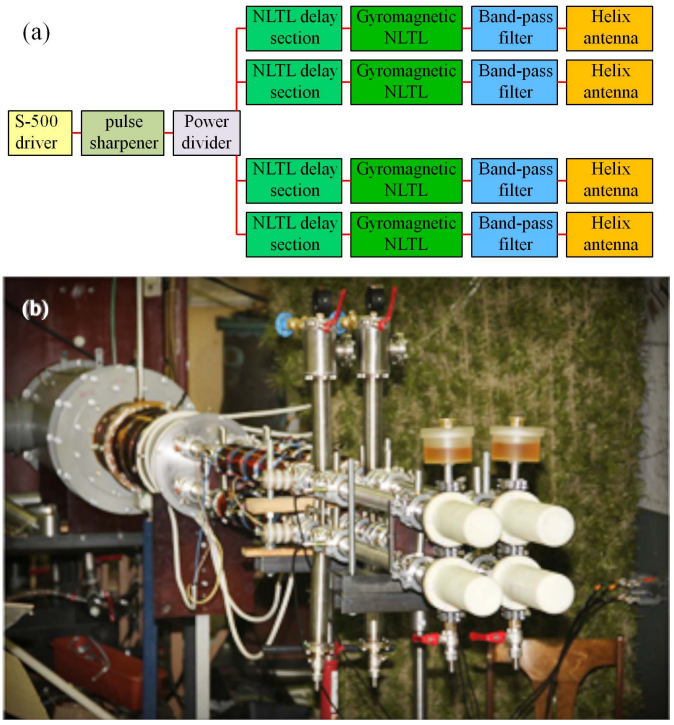

Fig. 18. (a) General schematic of the four-channel high power RF based on gyromagnetic NLTL (a) general schematic and (b) overall view. Adapted from [52], with the permission of AIP Publishing.

while the other three were used for optimal RF generation (about 400 mm of the ferrite filling).

The effect of the ferrite temperature on the RF phase between channels was also evaluated. For this purpose, two NLTLs in a vertical pair were heated simultaneously by solenoids to temperatures not higher than 50 °C. It was observed that the delay in the heated NLTLs underwent a decrease of approximately a quarter-period of oscillations or higher with respect to nonheated NLTLs. This experimental result showed an increase in the shock front velocity for heated NLTLs indicating that the effective magnetic permeability corresponding to the shock front wave inside the NLTL is a decreasing function of the temperature.

Another work using four gyromagnetic NLTLs in the synchronized operation is reported in [53]. The test results confirmed that using this configuration is possible to achieve the increase of flux power density in 16 times against that a single line. The high-voltage signals produced a pulse amplitude of −175 kV at a modulation depth of RF oscillations to 50% and an effective frequency around 4 GHz. The electric field strength achieved 250 kV/m at a distance of 3 m from the antenna.

The energy compression achieved with a high-voltage sub-nanosecond pulse generator which used a ferrite-filled gyromagnetic NLTL is reported in [54]. This system offered technical solution for pulse rise time reduction from 2 ns to 180 ps, increasing the voltage pulse amplitude from −185 to −325 kV.

VI. Discussion

An overview of relevant frequency and power limits achieved in experimental results with different types of NLTLs currently reported in the literature is shown in Table I. The examination of the constraints related to the materials is discussed in what follows.

TABLE I
Overview of Relevant Experimental Results With NLTLs

Structure Type	Key Material	Input Pulse (kV)	Frequency Range (GHz)	Output Peak Power	Ref.
CPW	HBV diode	0.008	231 - 247.5	10 mW	[7]
PCB	Varactor diode	0.02	0.12 – 0.25	98 W	[37]
Parallel Plate	Blocks of $Sr_{0.4}Ba_{0.6}TiO_3$	14	0.25 – 0.40	15.6 MW	[19]
PCB	Ceramic Capacitor	30	0.01 – 0.09	12 MW	[37]
Coaxial	Ferrite	30 – 50	0.20 – 2.00	20 MW	[30]
Coaxial	Ferrite (NiZn)	260	0.95 – 1.45	100 MW	[32]
Coaxial	Ferrite (YIG)	3 – 6	1.70 – 1.80	200 kW	[49]
Coaxial	Ferrite	30 – 50	2 – 6	1.3 MW	[50]
Coaxial	Ferrite (NiZn)	30	2 - 4	30 MW	[48]
Coaxial	Ferrite (NiZn)	150 – 270	0.60 – 1.00	3 GW	[47]
Coaxial	Ferrite (NiZn)	200	2.0 – 2.20	200 MW	[52]

A. Constraints of NLTLs Built With Semiconductor Materials

NLTLs built in CPW structures produced higher frequency oscillations, however, the miniaturized design showed a low-power handling capability [7]. The Schottky diodes used to build this line provided very low values of capacitance (around fF) providing oscillations around 240 GHz. To achieve higher frequencies, the dimensional reduction of the diode junction capacitance is required, but this is limited by the capability of the technological process of manufacture. On the other hand, the low reverse breakdown voltage of the Schottky diodes determined power level limitation. This line showed losses due to skin effect in the semiconductor and layout parasitic impedances associated with the high-frequency operation.

The capacitive NLTLs assembled in a PCB using varactor diodes have their performance limited by the maximum reverse breakdown voltage of the varactor. The operating frequency (9) is related to the minimum capacitance value provided by the varactor. The maximum frequency is around 300 MHz, since the stray impedances of the PCB is of order of several pF for a minimum capacitance value provided by the commercial available varactors (pF) and of tens of nH for a minimum inductance provided by the inductors formed on the PCB track layers [29].

B. Constraints of NLTLs Built With Ferroelectric Materials

The use of ferroelectric ceramic materials to build high-voltage NLTLs was reported in [19], [33], [34], [35], and [37], showing that the operational frequency is limited to 400 MHz. The best result achieved for RF generation using NLTLs built with nonlinear dielectric ceramics was reported in [19] using ceramics blocks based on barium and strontium titanate. These surveys have demonstrated that: 1) high-voltage values (around tens of kilovolts) are needed to access the nonlinear behavior of the relative permittivity; 2) the intrinsic temperature dependence behavior of the relative permittivity is a critical parameter; and 3) the dielectric loss was the main constraint for ferroelectric materials, since it can prevent the RF generation. Furthermore, the difficulty of coupling the RF pulse from the nonlinear lines efficiently into a linear resistive load is well known and is caused, primarily, by the voltage dependence of the line impedance [3], [55].

The analysis of the results obtained with capacitive NLTLs built with ferroelectric ceramics indicates the need of new research on ferroelectric materials to find materials with low dielectric losses at frequencies above 400 MHz. Considering that chemically different perovskites display very different ferroelectric behavior, Benedek and Fennie [56] and Mulder *et al.* [57] reported the connection between structural distortions and the ferroelectricity in perovskite oxides. Since prototypical ferroelectrics, such as BaTiO3 and PbTiO3, do not have structures with octahedral rotation distortions, the authors suggested that the design of new ferroelectric materials should pay attention to the structural stability (tolerance factor) in such a way to avoid the ferroelectricity suppression caused by octahedral rotation distortions. Using this approach, the research on different ferroelectric compositions could reveal useful materials to build NLTLs.

Another non-ferroelectric materials that also exhibit the nonlinear behavior of the relative permittivity with the applied electrical field is the bismuth zinc niobate (BZN) [58], [59]. BZN compounds are advantageous over ferroelectric materials due to the temperature-stable behavior of the relative permittivity [58]. Several researches have analyzed the correlation between the physical–chemical properties and electrical characteristics of bulk [60], [61] and thin-film BZN ceramics [62], [63]. There are two main phases in the BZN system [57]: 1) a cubic pyrochlore phase $Bi_{3/2}ZnNb_{3/2}O_7$, called α-BZN phase, with $\varepsilon_r \cong 150$ and temperature coefficient of ε_r around -400 ppm/°C and 2) a low-symmetry-structure with monoclinic zirconolite-like pyrochlore phase $Bi_2Zn_{2/3}3Nb_{4/3}O_7$, called β-BZN phase, with $\varepsilon_r \cong 80$ and temperature coefficient of ε_r around $+200$ ppm/°C. Then, from the mixture of the phases, it may be possible to achieve composites with a zero-coefficient temperature. Wang [61] reported the investigation of microwave dielectric properties for bulky samples of a BZN-based material $[(Bi_{1.92}Ca_{0.08})(Zn_{0.64}\ Nb_{1.36})O_7]$ that showed a relative permittivity of 76, loss tangent of 0.0013 and temperature coefficient of ε_r of 272 ppm/°C. Research on BZN ceramic thin films with low losses ($\sim 5 \times 10^{-4}$ at 1 MHz) and large tunability (55%) is discussed in [59]. Since nanosize materials are known to have properties that are very different from their bulk counterparts, studies on a possible nonlinear behavior of relative permittivity of BZN bulk materials need to be investigated.

C. Constraints of NLTLs Built With Ferrimagnetic Materials

Some characteristics of ferrites have decisive impact on the performance of gyromagnetic NLTLs: the initial relative magnetic permeability (μ_{in}), the coercivity (H_C), the saturation magnetization (B_S), the microwave dielectric losses, and the temperature dependence of magnetics properties.

The maximum operating frequency of gyromagnetic NLTLs is of the order of few gigahertz. The initial relative magnetic permeability of the ferrite contributes to the operating frequency (14), although the frequency is mainly affected by the axial magnetic polarization and the amplitude of the input field [64]. On the other hand, care must be taken to not exceed the breakdown voltage of the ferrite.

The dielectric loss value of commercially available ferrites is typically stated in their datasheet, but the magnetic loss is generally unknown. Experiments with gyromagnetic NLTLs using ferrites with different chemical compositions (NiZn and MnZn) were conducted in [48]. The investigation about the correlation between magnetic losses and the amplitude of output oscillations were made by analyzing the measurement of the ferrite linewidth. For distinct lines built with NiZn ferrites with different chemical compositions, the amplitude of microwave oscillations is higher for the NiZn ferrites with narrower linewidths. The line built with MnZn ferrites did not produce microwave oscillations, although these ferrites have shown values of linewidth lower than for NiZn ferrites. In this case, however, the low value of resistivity of MnZn ferrites prevented the generation of microwave oscillations (5–8 orders of magnitude lower than for NiZn samples) [48].

The efficiency of gyromagnetic NLTLs is strongly related to magnetic losses of the ferrite materials. The parallel arrangement of four gyromagnetic NLTLs was reported in [52] as a way to improve the device efficiency. This research also investigated the connection between the efficiency and the physical dimension of the ferrite geometry (filling factor), concluding that the efficiency could be maximized by an optimal arrangement of ferrite dimensions, bias magnetic field and the amplitude of the incident pulse.

Due to high-voltage oscillations, gyromagnetic NLTLs require the use of electric insulation to prevent breakdown, as illustrated by different types of insulator investigated in [32], [47], and [48]. The efficiency of the gyromagnetic lines is affected by the insulator due to its dielectric properties [47].

The temperature-dependent behavior of gyromagnetic NLTL's performance was reported in [50]. The unstable behavior of the magnetic properties of the ferrites is responsible for the variation in the oscillations (amplitude and frequency). Gyromagnetic NLTLs are also subject to the temperature rise caused by heat dissipation due to resistive and magnetic switching losses in the ferrites operating under pulsed repetition mode.

The development of new ferrimagnetic materials that present stable behavior with temperature of magnetic

TABLE II
PERCENTAGE CHANGE OF CAPACITANCE IN CAPACITIVE NLTLS

Element	Percentage Change of Capacitance	Output Frequency	Ref.
Varactor diode	74 % (from 26 to 6.8 pF)	130 GHz	[6]
Schottky diode	93 % (from 455 to 30 pF)	100 MHz	[15]
Varactor diode	77 % (from 56 to 13 pF)	33 MHz	[23]
Ceramic capacitor	91 % (from 8 to 0.7 pF)	16 MHz	[25]
Schottky diode	89 % (from 380 to 40 pF)	23 MHz	[25]
Varactor diode	62 % (from 570 to 50 pF)	250 MHz	[37]
Ceramic capacitor	81 % (from 1 to 0.38 nF)	4 MHz	[39]

TABLE III
REQUIRED PROPERTIES OF NONLINEAR DIELECTRIC MATERIALS

Property	Required Values	Effects on NLTL Performance
High nonlinearity behavior of relative permittivity with applied voltage	Percentage change of capacitance with applied voltage should be higher than 62 % [37]	High operating frequency
Medium to low values of relative permittivity [33]	To allow the construction of nonlinear capacitors with values around pF (depending on the size of capacitor)	High operating frequency
Low dielectric losses (high relaxation frequency of electric dipoles [33])	Higher than 1 GHz	High operation frequency and higher RF conversion efficiency

properties is clearly needed. The research of gyromagnetic NLTLs using nickel–zinc–cobalt ferrites would probably provide a more stable temperature behavior because cobalt is a bivalent cation that has an ionic radius similar in size to the zinc and nickel atoms and also has the highest Curie temperature among the chemical elements too. However, the investigation about the effect of the cobalt addition on the magnetic properties and as result on the performance of the NLTL is also required.

D. Required Characteristics of New Materials

The nonlinearity of capacitive elements is an important characteristic which enables the RF generation in capacitive NLTLs. Table II presents a summary of the nonlinear capacitive behavior discussed in different experiments reported in the literature. It can be observed that the construction of capacitive NLTLs using nonlinear components with low values of capacitance allows the generation of high frequencies oscillations [see (9)]. Furthermore, the wide operating range of the capacitance is essential to produce oscillations with high values of peak amplitude and VMD. The generation of RF oscillations was observed for a percentage change of capacitance values higher than 62% [37].

Another import characteristic of nonlinear dielectric materials used in capacitive NLTLs is the dielectric losses that occur in dielectric materials due to the relaxation frequency of electrical dipoles and could prevent the RF generation. In [33], the relaxation frequency of barium strontium titanate is estimated as 1 GHz. The dielectric strength (breakdown voltage) will place a limit on the maximum power handling capability. The main properties of nonlinear dielectric material and their influence on the performance of the capacitive NLTLs are listed in Table III.

In the literature, experiments with gyromagnetic NLTLs reported the use of NiZn, MnZn, and YIG ferrites. Better performances were achieved with NiZn ferrites, which are characterized by relative permeabilities in the upper hundreds, saturation magnetizations around 3500 G and high resistivity ($>10^5$ Ωm) [48].

TABLE IV
REQUIRED PROPERTIES OF FERRIMAGNETIC MATERIALS

Property	Effects on NLTL Performance
High relative permeability	High operating frequency
High resistivity	Low magnetic loss which allows high RF conversion efficiency
Narrow resonance linewidth	
Low saturation flux	Low magnetic field to achieve the saturation condition of the ferrite

The experimental results of a gyromagnetic line using YIG ferrites [49] showed that this line was driven by input voltages up to 6 kV, which is a lower value than the input voltage required to drive gyromagnetic NLTLs build with NiZn ferrites, indicating that the YIG ferrites presented a lower value of saturation magnetization. Additional investigations are required to accurately determine the ranges of values of properties of new materials. Mostly, the main properties of new ferrimagnetic materials and their influence on the performance of NLTLs are listed in Table IV.

The research on high-performance dielectric and ferrimagnetic materials is a great challenge since the desired properties depends on the structural phase transformation at Curie temperature, motivated by the fact that the use of cooling systems is an expensive and complex alternative, but may be needed for NLTLs operating at higher repetition rates (kHz). The internal heating due to thermal energy dissipation inside the materials should also affect the ferroelectric and ferrimagnetic properties. Moreover, the development of new materials should involve the characterization of their required properties as the

nonlinear behavior of relative permittivity and permeability, breakdown voltage, damping factor, dielectric losses, magnetic losses, and temperature stability.

VII. Conclusion

NLTLs have proven to be a robust, low cost, and fully solid-state technology for many applications in high-speed and wide bandwidth systems that require pulse sharpening and RF generation. Currently, the main achievements related to NLTLs reported in the literature can be classified as follows.

1) High-voltage capacitive NLTLs built with ferroelectric ceramic blocks based on strontium barium titanate have shown RF generation in frequencies of up to 300 MHz and peak power of 15 MW. Such lines required the application of high input pulses around tens of kilovolts, which allowed the access of the nonlinear dielectric behavior;
2) Low-voltage capacitive NLTLs which can be divided in two groups: 1) lines that were able to produce RF at frequencies up to 300 MHz with peak voltages up to 1000 V, assembled in a PCB using commercial inductors and varactors diodes and 2) lines with monolithic or coplanar geometry having small dimensions were able to operate in frequencies up to 300 GHz, but with extremely low power. In this case the limitation is related to the parasitic layout effects and minimum geometries of the varactor diodes;
3) Gyromagnetic NLTLs able to generate signals up to 6 GHz with peak power levels reaching hundreds of megawatts. These lines were built usually in a coaxial transmission line configuration and besides the application of high input pulses from tens to hundreds of kilovolts they require the use of a high current source to provide the axial biasing magnetization.

The performance of NLTLs is strongly related to the properties of nonlinear ferroelectric and ferrimagnetic materials that are employed. The improvement of the performance of NLTLs is still hampered by the lack of materials that present simultaneously nonlinear behavior, low losses, and thermal stability.

The literature reports the construction of capacitive NLTLs constructed with ferroelectric materials, in which the nonlinear behavior arises from the symmetry breaking (distortion) of the crystalline structure, which in turn is associated with the Curie temperature. However, the research on nonlinear dielectric materials that are non-ferroelectrics is a possibility to be investigated. The development of new nonlinear dielectrics materials for NLTLs requires materials that show the following characteristics:

1) nonlinear capacitance dependence on voltage, meaning a capacitance ratio above 62 percent [37], low values of capacitance are also needed to achieve higher frequency values;
2) low losses, avoiding the energy dissipation and, therefore increasing the conversion efficiency of the NLTL above 400 MHz up to microwave frequencies;
3) thermal stability of the relative permittivity, being a key factor to achieve a good performance of NLTLs in the range of the use.

The improvement of the performance of gyromagnetic NLTLs demands the development of new magnetic materials which present high initial saturation magnetization, lower saturation flux density, low losses at microwave frequencies, and the thermal stability in the range of use. Finally, the achievement of a stable behavior over a broader operating temperature range would allow the application of NLTLs in wider areas such as military and aerospace devices, which can involve pulse repetition of tens of kHz.

References

[1] M. S. Nikoo and S. M.-A. Hashemi, "New soliton solution of a varactor-loaded nonlinear transmission line," *IEEE Trans. Microw. Theory Techn.*, vol. 65, no. 11, pp. 4084–4092, Nov. 2017.
[2] M. S. Nikoo and S. M.-A. Hashemi, "Analysis of the power transfer to a nonlinear transmission line," *IEEE Trans. Microw. Theory Techn.*, vol. 65, no. 11, pp. 4073–4083, Nov. 2017.
[3] M. S. Nikoo, S. M.-A. Hashemi, and F. Farzaneh, "Theory of terminated nonlinear transmission lines," *IEEE Trans. Microw. Theory Techn.*, vol. 66, no. 1, pp. 91–99, Jan. 2018.
[4] E. Afshari and A. Hajimiri, "Nonlinear transmission lines for pulse shaping in silicon," *IEEE J. Solid-State Circuits*, vol. 40, no. 3, pp. 744–752, Mar. 2005.
[5] P. Indirayanti, W. Volkaerts, P. Reynaert, and W. Dehaene, "Picosecond pulse generation with nonlinear transmission lines in 90-nm CMOS for mm-wave imaging applications," in *Proc. 19th IEEE Int. Conf. Electron., Circuits, Syst. (ICECS)*, Seville, Spain, Dec. 2012, pp. 885–888.
[6] S. Hollung, J. Stake, L. Dillner, M. Ingvarson, and E. Kollberg, "A distributed heterostructure barrier varactor frequency tripler," *IEEE Microw. Guided Wave Lett.*, vol. 10, no. 1, pp. 24–26, Jan. 2000.
[7] X. Melique *et al.*, "12% efficiency and 9.5 dBm output power from InP-based heterostructure barrier varactor triplers at 250 GHz," in *IEEE MTT-S Int. Microw. Symp. Dig.*, Anaheim, CA, USA, vol. 1, Jun. 1999, pp. 123–126.
[8] A. S. Nagra and R. A. York, "Distributed analog phase shifters with low insertion loss," *IEEE Trans. Microw. Theory Techn.*, vol. 47, no. 9, pp. 1705–1711, Sep. 1999.
[9] H. Kim, S.-J. Ho, C.-C. Yen, K.-O. Sun, and D. W. V. D. Weide, "Balanced distributed-element phase shifter," *IEEE Microw. Wireless Compon. Lett.*, vol. 15, no. 3, pp. 147–149, Mar. 2005.
[10] D. S. Ricketts, X. Li, and D. Ham, "Electrical soliton oscillator," *IEEE Trans. Microw. Theory Techn.*, vol. 54, no. 1, pp. 373–382, Jan. 2006.
[11] M. Ponton, F. Ramirez, A. Suarez, and J. P. Pascual, "Analysis and design of soliton oscillators using harmonic balance," in *IEEE MTT-S Int. Microw. Symp. Dig.*, Boston, MA, USA, Jun. 2009, pp. 1485–1488.
[12] O. Wohlgemuth, M. J. W. Rodwell, R. Reuter, J. Braunstein, and M. Schlechtweg, "Active probes for 2-port network analysis within 70–230 GHz," in *IEEE MTT-S Int. Microw. Symp. Dig.*, Anaheim, CA, USA, vol. 4, Jun. 1999, pp. 1635–1638.
[13] K. Noujeim, G. Malysa, A. Babveyh, and A. Arbabian, "A compact nonlinear-transmission-line-based mm-wave SFCW imaging radar," in *Proc. 44th Eur. Microw. Conf.*, Rome, Italy, Oct. 2014, pp. 1766–1769.
[14] J. D. C. Darling and P. W. Smith, "High-power pulsed RF extraction from nonlinear lumped element transmission lines," *IEEE Trans. Plasma Sci.*, vol. 36, no. 5, pp. 2598–2603, Oct. 2008.
[15] D. M. French, B. W. Hoff, W. Tang, S. Heidger, J. Allen-Flowers, and D. Shiffler, "Nonlinear transmission line based electron beam driver," *Rev. Sci. Instrum.*, vol. 83, no. 12, pp. 123302-1–123302-4, Dec. 2012.
[16] B. W. Hoff, D. M. French, D. S. Simon, P. D. Lepell, T. Montoya, and S. L. Heidger, "High current nonlinear transmission line based electron beam driver," *Phys. Rev. Accel. Beams*, vol. 20, no. 10, pp. 100401-1–100401-8, Oct. 2017.
[17] I. V. Romanchenko, V. V. Rostov, A. V. Gunin, and V. Y. Konev, "High power microwave beam steering based on gyromagnetic nonlinear transmission lines," *J. Appl. Phys.*, vol. 117, pp. 214907-1–214907-6, Jun. 2015.
[18] D. V. Reale, J. M. Parson, A. A. Neuber, J. C. Dickens, and J. J. Mankowski, "Investigation of a stripline transmission line structure for gyromagnetic nonlinear transmission line high power microwave sources," *Rev. Sci. Instrum.*, vol. 87, no. 3, pp. 034706-1–034706-5, Mar. 2016.

[19] H. Ikezi, J. S. DeGrassie, and J. Drake, "Soliton generation at 10 MW level in the very high frequency band," *Appl. Phys. Lett.*, vol. 58, no. 9, pp. 986–987, Mar. 1991.

[20] J. O. Rossi, P. N. Rizzo, and F. S. Yamasaki, "Prospects for applications of hybrid lines in RF generation," in *Proc. IEEE Int. Power Modulator High Voltage Conf.*, Atlanta, GA, USA, May 2010, pp. 632–635.

[21] N. S. Kuek, A. C. Liew, E. Schamiloglu, and J. O. Rossi, "Pulsed RF oscillations on a nonlinear capacitive transmission line," *IEEE Trans. Dielectr. Electr. Insul.*, vol. 20, no. 4, pp. 1129–1135, Aug. 2013.

[22] Q. R. Marksteiner, B. Carlsten, and S. Russel, "Numerical calculations of RF efficiency from a soliton generating nonlinear transmission line," *J. Appl. Phys.*, vol. 106, no. 11, pp. 113306-1–113306-7, Dec. 2009.

[23] E. G. L. Rangel, J. J. Barroso, J. O. Rossi, F. S. Yamasaki, L. P. S. Neto, and E. Schamiloglu, "Influence of input pulse shape on rf generation in nonlinear transmission lines," *IEEE Trans. Plasma Sci.*, vol. 44, no. 10, pp. 2258–2267, Oct. 2016.

[24] P. W. Smith, "Nonlinear pulsed power," in *Transient Electronics—Pulsed Circuit Technology*, 1st ed. West Sussex, U.K.: Wiley, 2002, ch. 8, p. 247.

[25] J. M. Elizondo-Decanini *et al.*, "Soliton production with nonlinear homogeneous lines," *IEEE Trans. Plasma Sci.*, vol. 43, no. 12, pp. 4136–4142, Dec. 2015.

[26] J. O. Rossi, F. S. Yamasaki, E. Schamiloglu, J. J. Barroso, and U. C. Hasar, "Operation analysis of a novel concept of RF source known as gyromagnetic line," in *Proc. SBMO/IEEE MTT-S Int. Microw. Optoelectron. Conf. (IMOC)*, Águas de Lindoia, Brazil, Aug. 2017, pp. 1–4.

[27] S. J. F. Chadwick, N. Seddon, and S. Rukin, "A novel solid-state HPM source based on a gyromagnetic NLTL and SOS-based pulse generator," in *Proc. IEEE Pulsed Power Conf.*, Chicago, IL, USA, Jun. 2011, pp. 178–181.

[28] F. S. Yamasaki, E. Schamiloglu, J. O. Rossi, and J. J. Barroso, "Simulation studies of distributed nonlinear gyromagnetic lines based on LC lumped model," *IEEE Trans. Plasma Sci.*, vol. 44, no. 10, pp. 2232–2239, Oct. 2016.

[29] J. O. Rossi, L. P. S. Neto, F. S. Yamasaki, J. J. Barroso, E. G. L. Rangel, and E. Schamiloglu, "High-voltage soliton generation with nonlinear lumped varactor diode lines," in *Proc. 18th Symp. Oper. Appl. Areas Defense*, São José dos Campos, Brazil, Sep. 2016, pp. 22–25.

[30] N. Seddon, C. R. Spikings, and J. E. Dolan, "RF pulse formation in nonlinear transmission lines," in *Proc. 16th IEEE Int. Pulsed Power Conf.*, Albuquerque, NM, USA, Jun. 2007, pp. 678–681.

[31] P. D. Coleman, J. J. Borchardt, J. A. Alexander, J. T. Williams, and T. F. Peters, "Characterization of a synchronous wave nonlinear transmission line," in *Proc. IEEE Int. Pulsed Power Conf.*, Chicago, IL, USA, Jun. 2011, pp. 173–177.

[32] D. M. French and B. W. Hoff, "Spatially dispersive ferrite nonlinear transmission line with axial bias," *IEEE Trans. Plasma Sci.*, vol. 42, no. 10, pp. 3387–3390, Oct. 2014.

[33] G. Branch and P. W. Smith, "Fast-rise-time electromagnetic shock waves in nonlinear, ceramic dielectrics," *J. Phys. D: Appl. Phys.*, vol. 29, no. 8, pp. 2170–2178, Mar. 1996.

[34] M. P. Brown and P. W. Smith, "High power, pulsed soliton generation at radio and microwave frequencies," in *11th IEEE Int. Pulsed Power Conf. Dig. Tech. Papers*, Baltimore, MD, USA, vol. 1, Jun./Jul. 1997, pp. 346–354.

[35] D. M. French, B. W. Hoff, S. Heidger, and D. Shiffler, "Dielectric nonlinear transmission line," in *Proc. IEEE Int. Pulsed Power Conf.*, Chicago, IL, USA, Jun. 2011, pp. 341–345.

[36] C. R. Wilson, M. M. Turner, and P. W. Smith, "Electromagnetic shock-wave generation in a lumped element delay line containing nonlinear ferroelectric capacitors," *Appl. Phys. Lett.*, vol. 56, pp. 2471–2473, Jun. 1990.

[37] J. Darling, "High power pulsed RF generation by soliton type oscillation on nonlinear lumped element transmission lines," Ph.D. dissertation, Eng. Sci. Dept., Oxford Univ., Oxford, U.K., 2009.

[38] S. Ibuka, T. Miyazawa, A. Ishii, and S. Ishii, "Fast high voltage pulse generator with nonlinear transmission line for high repetitive operation," in *10th IEEE Int. Pulsed Power Conf. Dig. Tech. Papers*, Albuquerque, NM, USA, vol. 2, Jul. 1995, pp. 1365–1370.

[39] L. P. S. Neto, J. O. Rossi, J. J. Barroso, and E. Schamiloglu, "High-power RF generation from nonlinear transmission lines with barium titanate ceramic capacitors," *IEEE Trans. Plasma Sci.*, vol. 44, no. 12, pp. 3424–3431, Dec. 2016.

[40] M. J. W. Rodwell, M. Kamegawa, R. Yu, M. Case, E. Carman, and K. S. Giboney, "GaAs nonlinear transmission lines for picosecond pulse generation and millimeter-wave sampling," *IEEE Trans. Microw. Theory Techn.*, vol. 39, no. 7, pp. 1194–1204, Jul. 1991.

[41] J. Stake, A. Malko, T. Bryllert, and J. Vukusic, "Status and prospects of high-power heterostructure barrier varactor frequency multipliers," *Proc. IEEE*, vol. 105, no. 6, pp. 1008–1019, Jun. 2017.

[42] H. Shi, W.-M. Zhang, C. W. Domier, N. C. Luhmann, Jr., L. B. Sjogren, and H.-X. L. Liu, "Novel concepts for improved nonlinear transmission line performance," *IEEE Trans. Microw. Theory Techn.*, vol. 43, no. 4, pp. 780–789, Apr. 1995.

[43] M. G. Case, "Nonlinear transmission lines for picosecond pulse, impulse and millimeter-wave harmonic generation," Ph.D. dissertation, Dept. Elect. Comput. Eng., California Univ., Santa Barbara, CA, USA, 1993.

[44] V. V. Rostov, N. M. Bykov, D. N. Bykov, A. I. Klimov, O. B. Kovalchuk, and I. V. Romanchenko, "Generation of subgigawatt RF pulses in nonlinear transmission lines," *IEEE Trans. Plasma Sci.*, vol. 38, no. 10, pp. 2681–2685, Oct. 2012.

[45] S. Ito. Basics of ferrite and noise countermeasures. TDK Corporation, Tokyo, Japan. Accessed: Nov. 22, 2017. [Online]. Available: https://product.tdk.com/en/products/emc/guidebook/eemc_basic_06.pdf

[46] A. M. Belyantsev and A. B. Kozyrev, "Influence of local dispersion on transient processes accompanying the generation of RF radiation by an electromagnetic shock wave," *Tech. Phys.*, vol. 43, no. 1, pp. 80–85, Jan. 1998.

[47] I. V. Romanchenko, V. V. Rostov, A. V. Gunin, and V. Y. Konev, "Gyromagnetic RF source for interdisciplinary research," *Rev. Sci. Instrum.*, vol. 88, pp. 024703-1–024703-5, Feb. 2017.

[48] J.-W. B. Bragg, J. C. Dickens, and A. A. Neuber, "Material selection considerations for coaxial, ferrimagnetic-based nonlinear transmission lines," *J. Appl. Phys.*, vol. 113, no. 6, pp. 064904-1–064904-4, Feb. 2013.

[49] D. V. Reale, D. Mauch, J. M. Johnson, A. A. Neuber, J. C. Dickens, and J. J. Mankowski, "Radiation from SiC PCSS driven gyromagnetic nonlinear transmission line high power microwave source," in *Proc. IEEE Int. Power Modulator High Voltage Conf. (IPMHVC)*, Santa Fe, NM, USA, Jun. 2014, pp. 123–125.

[50] J.-W. B. Bragg, J. Dickens, and A. Neuber, "Investigation into the temperature dependence of ferrimagnetic nonlinear transmission lines," *IEEE Trans. Plasma Sci.*, vol. 40, no. 10, pp. 2457–2461, Oct. 2012.

[51] I. V. Romanchenko, V. V. Rostov, V. P. Gubanov, A. S. Stepchenko, A. V. Gunin, and I. K. Kurkan, "Repetitive sub-gigawatt RF source based on gyromagnetic nonlinear transmission line," *Rev. Sci. Instrum.*, vol. 83, no. 7, pp. 074705-1–074705-6, Jul. 2012.

[52] I. V. Romanchenko *et al.*, "Four channel high power RF source with beam steering based on gyromagnetic nonlinear transmission lines," *Rev. Sci. Instrum.*, vol. 88, no. 5, pp. 054703-1–054703-6, May 2017.

[53] M. R. Ul'maskulov *et al.*, "Coherent summation of radiation from four-channel shock-excited RF source operating at 4 GHz and a repetition rate of 1000 Hz," *IEEE Trans. Plasma Sci.*, vol. 45, no. 10, pp. 2623–2628, Oct. 2017.

[54] M. R. Ulmaskulov *et al.*, "Energy compression of nanosecond high-voltage pulses based on two-stage hybrid scheme," *Rev. Sci. Instrum.*, vol. 88, no. 4, p. 045106, Apr. 2017.

[55] P. W. Smith, "Pulsed, high power, RF generation from nonlinear dielectric ladder networks—Performance limits," in *Proc. IEEE Pulsed Power Conf.*, Chicago, IL, USA, Jun. 2011, pp. 167–172.

[56] N. A. Benedek and C. J. Fennie, "Why are there so few perovskite ferroelectrics?" *J. Phys. Chem. C*, vol. 117, no. 26, pp. 13339–13349, May 2013.

[57] A. T. Mulder, N. A. Benedek, J. M. Rondinelli, and C. J. Fennie, "Turning ABO_3 antiferroelectrics into ferroelectrics: Design rules for practical rotation-driven ferroelectricity in double perovskites and $A_3B_2O_7$ Ruddlesden–Popper compounds," *Adv. Funct. Mater.*, vol. 23, pp. 4810–4820, Oct. 2013.

[58] M. T. Sebastian, "Low temperature cofired ceramics," in *Dielectric Materials for Wireless Communication*, 8th ed. Oxford, U.K.: Elsevier, 2008, ch. 12, pp. 472–477.

[59] A. Ahmed, I. A. Goldthorpe, and A. K. Khandani, "Electrically tunable materials for microwave applications," *Appl. Phys. Lett.*, vol. 2, no. 1, Sep. 2015, Art. no. 011302.

[60] J. C. Nino, M. T. Lanagan, and C. Randall, "Phase formation and reactions in the Bi_2O_3–ZnO–Nb_2O_5–Ag pyrochlore system," *J. Mater. Res.*, vol. 16, pp. 1460–1464, May 2001.

[61] H. Wang, " Microwave and infrared dielectric response of monoclinic bismuth zinc niobate based pyrochlore ceramics with ion substitution in A site," *J. Appl. Phys.*, vol. 100, pp. 034109-1–034109-6, Aug. 2006.
[62] J. Park, J. Lu, S. Stemmer, and R. A. York, "Low-loss, tunable microwave capacitors using bismuth zinc niobate thin films," in *Proc. 14th IEEE Int. Symp. Appl. Ferroelectr.*, Aug. 2004, pp. 17–20.
[63] A. K. Tagantsev, J. Lu, and S. Stemmer, "Temperature dependence of the dielectric tunability of pyrochlore bismuth zinc niobate thin films," *Appl. Phys. Lett.*, vol. 86, pp. 032901-1–032901-4, Jan. 2005.
[64] I. V. Romanchenko and V. V. Rostov, "Frequency of high power RF-generation in nonlinear transmission lines with saturated ferrite," in *Proc. 16th Int. Symp. High Current Electron.*, Tomsk, Russia, 2010, pp. 521–524.

Elizete G. Lopes Rangel (M'18) received the B.Sc. degree in electronic engineering from Fundação Valeparaibana de Ensino, São José dos Campos, Brazil, in 1991, the M.S. degree in metrology from Pontifical Catholic University, Rio de Janeiro, Brazil, in 2005, and the Ph.D. degree in space engineering and technology from the National Institute for Space Research (INPE), São José dos Campos, in 2011.

Since 2005, she has been with INPE, where she is involved in activities related to the technological development in the aerospace area such as product assurance of satellite systems, metrological reliability of measurement systems, and qualification process of electronic components for satellites. Recently, she is dedicated to the research on nonlinear transmission lines for RF generation and the investigation of nonlinear dielectric and magnetic materials to improve the line performance.

José O. Rossi (M'05–SM'12) received the B.Sc. degree in electrical engineering from Campinas University, Campinas, Brazil, in 1982, the M.Sc. degree in electronics from the Technological Institute of Aeronautics (ITA), São José dos Campos, Brazil, in 1992, and the Ph.D. degree in engineering science from Oxford University, Oxford, U.K., in 1998.

He has been with the National Institute for Space Research (INPE), São José dos Campos, since 1983, where he focuses on pulsed power generators for microwave generation and plasma implantation surface treatments. From 1994 to 1998, he was involved in a Ph.D. program on pulsed power systems and transmission line pulse transformers at the Department of Engineering Science, Oxford University. From 2007 to 2008, he was a Visiting Scientist with the Department of Electrical and Computer Engineering, University of New Mexico, Albuquerque, NM, USA, where he was involved with research on dielectrics of high breakdown strength for compact energy storage systems. His current research interests include nonlinear transmission lines and high-voltage ceramic dielectrics used in the development of compact pulsed power supplies and RF generation sources for space, defense systems, and plasma surface processing applications.

Dr. José Rossi is a member of Brazilian Power Electronics and Physical Societies and a Consultant on research projects for the State of Sao Paulo Research Foundation (FAPESP), Brazil.

Joaquim J. Barroso received the B.S. degree in electronics engineering and the M.S. degree in plasma physics from the Technological Institute of Aeronautics (ITA), São José dos Campos, Brazil, in 1976 and 1980, respectively, and the Doctor degree in plasma physics from the National Institute for Space Research (INPE), São José dos Campos, in 1988.

From 1989 to 1990, he was a Visiting Scientist at the Massachusetts Institute of Technology, Cambridge, MA, USA. At INPE, he is involved in the design and construction of high-power microwave tubes. He is currently a Visiting Professor at ITA. His current research interests include microwave electronics, electromagnetics, and metamaterials.

Fernanda S. Yamasaki (M'15) was born in Cruzeiro, Brazil, in 1988. She received the B.Sc. degree in telecommunication technology from the University of Campinas, Limeira Campus, Brazil, in 2010, and the M.Sc. and D.Sc. degrees in engineering and space technology from the National Institute for Space Research (INPE), Sao Jose dos Campos, Brazil, in 2013 and 2017, respectively.

Since 2010, she has been with INPE, focusing on nonlinear transmission lines for RF generation. From 2011 to 2013, she developed Spice models to simulate nonlinear dielectric lines. Her current research interests include the study of RF generation using nonlinear gyromagnetic lines for applications in space technologies.

Mr. Yamasaki was also awarded in 2015 with the Best Student Paper on gyromagnetic line simulations at the 2015 IEEE International Pulsed Power Conference.

Edl Schamiloglu (M'90–SM'95–F'02) received the B.S. degree in applied physics and the M.S. degree in plasma physics from Columbia University, New York City, NY, USA, in 1979 and 1981, respectively, and the Ph.D. degree in engineering (minor in mathematics) from Cornell University, Ithaca, NY, USA, in 1988.

He joined the University of New Mexico, Albuquerque, NM, USA, as an Assistant Professor, in 1988 and he is currently a Distinguished Professor of electrical and computer engineering and directs the Pulsed Power, Beams, and Microwaves Laboratory. He is also the Associate Dean of Research with the School of Engineering. He has co-edited *Advances in High Power Microwave Sources and Technologies* (Piscataway, NJ: IEEE, 2001) (with R. J. Barker). He has co-authored *High Power Microwaves*, third Edition (CRC Press, Boca Raton, FL, 2016) (with J. Benford and J. Swegle) and over 135 refereed journal papers and over 225 reviewed conference papers. He holds six patents.

Dr. Schamiloglu was awarded the 2013 IEEE Nuclear and Plasma Sciences Society's Richard F. Shea Distinguished Member Award, the 2014 IEC (International Electrotechnical Commission) 1906 Award Recognizing an Expert's Exceptional Current Achievements, and the 2015 IEEE NPSS Peter Haas Award, which recognizes outstanding contributions to pulsed power technology resulting from an individual's continued effort to develop programs of research education, and information exchange that are the basis for progress in pulsed power.